

## ANALYSIS OF HORN RADIATION PATTERN USING UTD EDGE AND CORNER DIFFRACTION

M. Ali and S.-O. Park

Korea Advanced Institute of Science and Technology  
119 Monjiro Yuseong-Gu, Daejeon 305-732, Korea

S. Sanyal

Department of Electronics & Electrical Communication Engineering  
Indian Institute of Technology  
Kharagpur 721-302, India

**Abstract**—Finite edge geometrical theory of diffraction (FEGTD) approach is a new and latest improvement in GTD technique. This FEGTD technique is applied to the  $E$ -plane horn radiation problems with spherical source excitation. The radiation patterns obtained with the FEGTD approach are found to be in good agreement with measured results.

### 1. INTRODUCTION

Application of the geometrical theory of diffraction (GTD) to predict accurately the far side lobes and back lobes of an antenna has been the subject of interest for quite some time as it is a good canonical problem which has a broad range of low response in the backward (LRB) directions [1]. Keller's GTD [2] and later the uniform theory of diffraction (UTD) [3] and the uniform asymptotic theory (UAT) [4, 5] have been applied to horn antennas [6–12]. In the year 2010, finite edge GTD (FEGTD) technique is developed and applied to compute  $H$ -plane horn radiation pattern in [13]. The FEGTD approach in [13] shows improved agreement with measured results compared to earlier GTD formulations in [8, 9] for  $H$ -plane horn radiation pattern. This is a pure GTD formulation that gives good results in all regions an attractive proposition because it gives the physical inside of the

problem and it would require insignificant computer time and resources (as compared to purely numerical technique).

The earliest work on  $E$ -plane horn radiation pattern using Keller's GTD was by Russo et al. [6]. They approximated the pyramidal horn by a dihedral corner reflector excited by a magnetic line source and then obtained its  $E$ -plane far field radiation pattern. A more comprehensive analysis of the  $E$ -plane radiation pattern was carried out by Yu et al. in [7]. Their analysis included the multiply reflected images and as a result, they obtained continuous far field  $E$ -plane patterns at all angle. The computed  $E$ -plane pattern in the later investigation [9–11] however, shows no improvement over that obtained as early as 1966 in [7]. A fundamental limitation in [7] was the approximation (up to  $K^{-1/2}$  term) of the line source at the edge and the images to be isotropic. This limitation does not exist in UAT. UAT applied to determine near field [10] also gives term of order  $K^{-1/2}$  which in general differs from that of UAT [14–16]. Further refinement in predicting the far out side lobes ripples, better than 1 dB at 35 dB below reference, in the  $E$ -plane radiation pattern was carried out by Sanyal and Bhattacharyya in [12].

From all this discussions, it is seen that GTD formulation have till now failed in the backward broad range of low response regions because the finiteness of the edges were not incorporated in the diffraction coefficient used. The problem of diffraction by the edge of an infinite half-plane/wedge is a canonical problem in GTD. GTD offers an asymptotic solution to this problem. Because, of this the GTD formulations having these canonical problem as their base have failed, wherever finiteness of the edges plays an important rule. In GTD formulation, finite edge would mean a corner discontinuity. In order to incorporate this finite effect in the horn problem, corner diffraction needs to be considered.

Recently, UTD technique has been applied to analysis of complex antenna around the scatterer in [17, 18]. An approximate, UTD based ray solutions are applied to analysis high frequency electromagnetic (EM) wave radiation/coupling mechanisms for antennas on or near a junction between two different thin planar slabs on ground plane in [19]. But corner diffraction has not been used explicitly in there computations.

In this paper,  $E$ -plane horn radiation patterns are computed using FEGTD technique. Firstly, a two dimensional (2D) model of the horn using spherical source at the apex of a dihedral corner reflector formed by inclined half-planes (see Fig. 1(b)) is considered and UTD of [20] is applied to compute the field. Then higher order fields are computed by taking the account of multiply diffracted rays from its edge (see

Fig. 5) and apex. The apex is considered as a wedge (see Fig. 6(b)) of wedge angle  $2\theta_E$ . Finally, corner diffractions arising in the case of three dimension (3D) horn model are added to take the accounts of finiteness of the horn edges. The computed patterns are compared with the measured patterns.

## 2. HORN RADIATION PROBLEM

Geometry of a pyramidal horn along with its top ( $H$ -plane), side ( $E$ -plane) and front view are shown in Fig. 1. The  $TE_{10}$  mode at the waveguide horn junction gives rise to a tube of rays and the diverging wavefront shown emerging from the aperture in Fig. 2. The axial ray, which is surrounded by the tube of rays, coincides with the  $Z$ -axis. The horn  $E$  and  $H$ -planes intersect the principle direction of the wavefront surface. These planes intersect at a point  $z_0$  on the wavefront. The principle radii of curvature of the diverging phase front are  $(\rho_E, \rho_H)$ . Along the  $E$  and  $H$ -planes the phase variations of the diverging wavefront are coincident with those of spherical source excitations at  $S_H$  and  $S_E$  respectively.

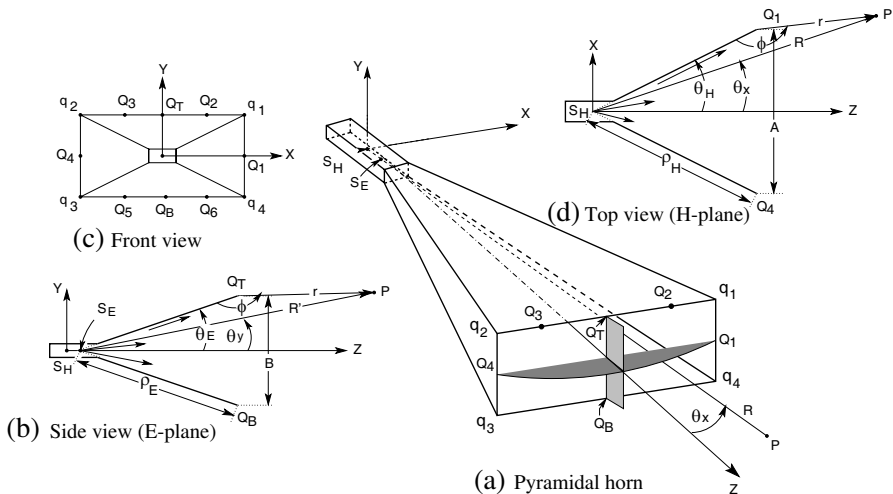


**Figure 1.** Geometry of a pyramidal horn antenna.

For the computation of  $E$ -plane radiation pattern, apex ( $S_E$ ) is considered as the origin of the coordinate system. When the effects of top and bottom  $E$ -edges (edges perpendicular to the principal  $E$ -plane) are computed the corner reflector is assumed to be excited by an anisotropic spherical source at the vertex  $S_E$  and when the effects

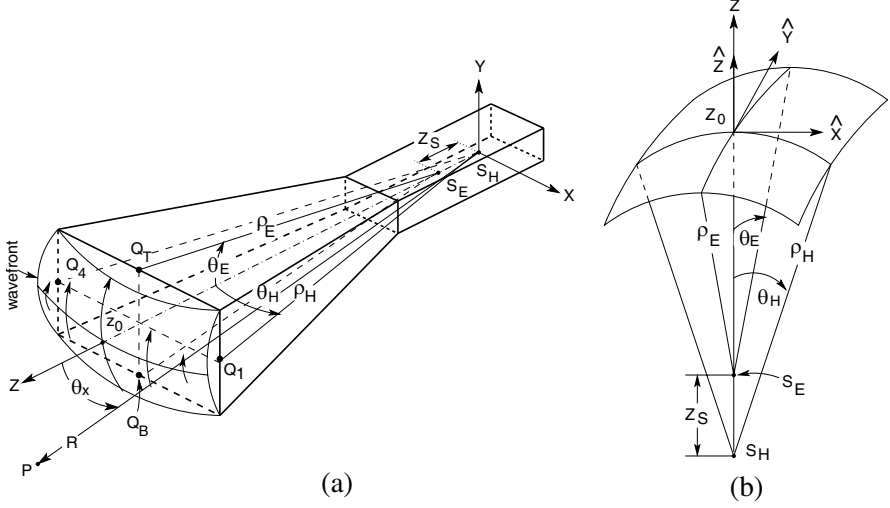


**Figure 2.** Diverging wavefront at the aperture of a pyramidal horn.

of side  $H$ -edges (edges parallel to the principal  $E$ -plane) are computed the corner reflector is assumed to be excited by an anisotropic spherical source at the vertex  $S_H$ . Rays from this source are assumed to have electric vector parallel to the corner reflector  $H$ -edges. The ray-optical expansion of this source field (GO field) in the  $H$ -plane is assumed to be given by

$$E^i = E_0 \cos \left( \frac{\pi}{A} \rho_H \cos \theta_H \tan \theta_x \right) \frac{\exp(-jkR)}{R} \quad (1)$$

which satisfies the boundary condition for the horn, i.e., the field  $E^i$  at  $(x = \pm A/2, -B/2 \leq y \leq B/2, z = \rho_H \cos \theta_H)$  is zero and the polarization is along  $Y$ -axis. This direct GO field ( $E^i(P)$ ) contributes in the  $H$ -plane and  $E$ -plane horn radiation patterns within angle  $|\theta_x| \leq \theta_H$  and  $|\theta_y| \leq \theta_E$  respectively. The angles are shown in Fig. 1.

## 2.1. Measurement Setup and Process

To validate the computation, computed results are compared with measurement. The schematic of measurement setup is shown in Fig. 3. It is a 4-axis fully automated measurement system in an anechoic chamber. The specifications of the anechoic chamber are given below

- Size:  $10 \text{ m}(L) \times 6 \text{ m}(W) \times 5 \text{ m}(H)$
- Frequency Rang:  $0.8 \sim 40 \text{ GHz}$

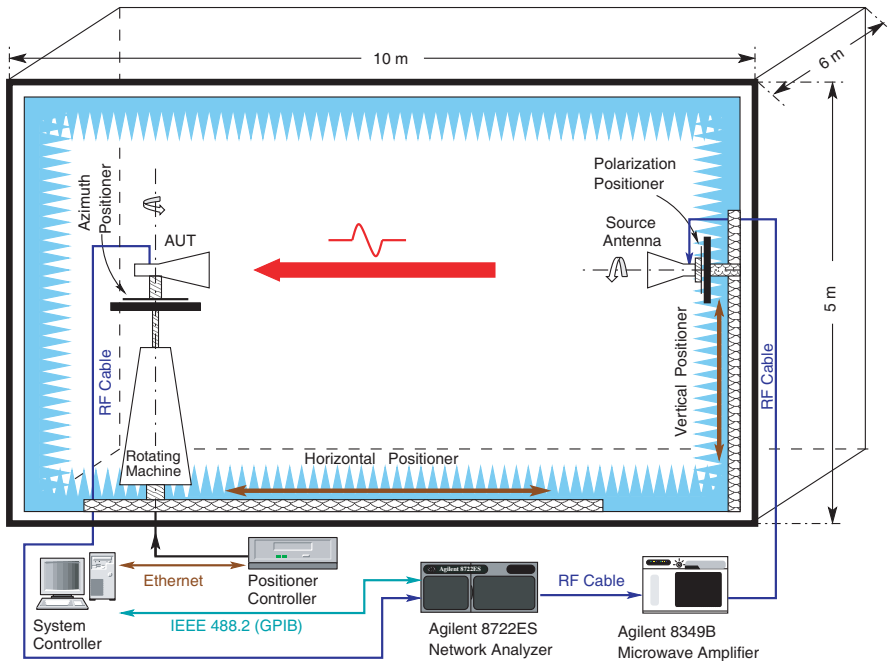


**Figure 3.** A schematic of measurement setup.

- Type: Rectangular
- Quiet Zone: 1 m @ 800 MHz
- Temperature:  $21 \pm 2^\circ\text{C}$
- Humidity:  $45 \pm 8\%$

A broadband double-ridged horn antenna is used in transmitting mode and the antenna under test (AUT) on a rotating machine is used in receiving mode as shown in the Fig. 3. The rotating machine rotates in one degree step and the fields captured by the AUT are recorded with respect to the angular position of the AUT. Graphical representation of the field with respect to angular position of the AUT is known as radiation pattern. These patterns of a horn antenna are measured for different frequencies.

## 2.2. Analysis of *E*-plane Horn Radiation Pattern by GTD (UTD) Method

The *Y-Z* plane is the *E*-plane, and it is explicitly shown in Fig. 1(b). The horn antenna is approximated by a dihedral corner reflector formed

by two infinite perfectly conducting, inclined half-planes and excited by a spherical source at the vertex  $S_E$  (Fig. 1). Edge diffraction from the mid point ( $Q_T$ ) of  $E$ -edge  $q_1q_2$  and edge diffraction from the mid point ( $Q_B$ ) of  $E$ -edge  $q_3q_4$  are shown in Fig. 4(a). Detailed geometry of  $E$ -edge diffraction for the calculation of  $E$ -plane horn radiation pattern is also shown in Fig. 4(b). The edge diffracted fields from the  $E$ -edges  $q_1q_2$  ( $E_{Q_T}^d$ ) and  $q_3q_4$  ( $E_{Q_B}^d$ ) are calculated using UTD of [3]. The spreading factor as well as phase function for the edge or wedge diffracted field are according to [3].

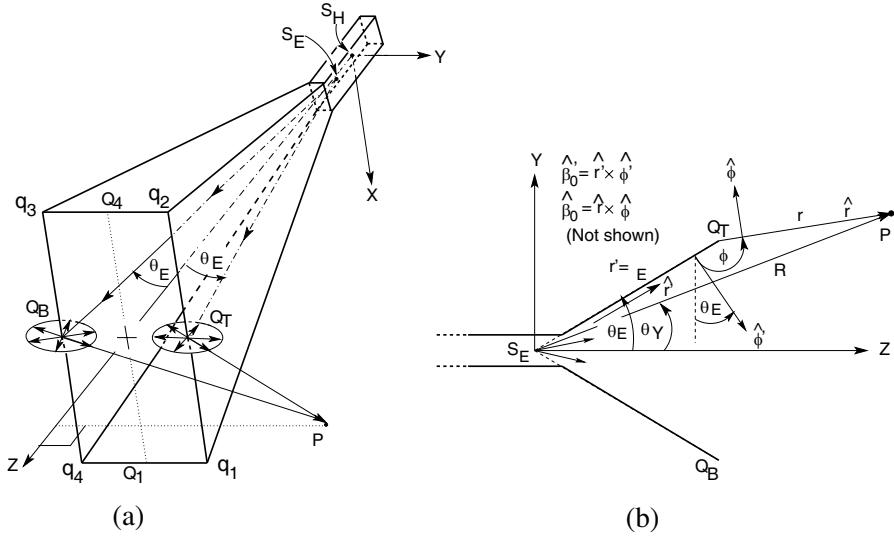


**Figure 4.**  $E$ -plane horn radiation pattern (a)  $E$ -edge diffractions, (b) Geometry of  $E$ -edge diffraction.

The multiply diffractions from  $E$ -edges are shown in Fig. 5. First order diffracted field ( $E_{Q_B}^d$ ) from the midpoint  $Q_B$  of edge  $q_3q_4$  incident on the midpoint  $Q_T$  of edge  $q_1q_2$  creates second order edge diffraction ( $E_{Q_T}^{2d}$ ). Similarly, first order edge diffracted field ( $E_{Q_T}^d$ ) from  $Q_T$  incident on  $Q_B$  creates second order edge diffraction ( $E_{Q_B}^{2d}$ ). Again, second order diffracted field ( $E_{Q_B}^{2d}$ ) from the midpoint  $Q_B$  of edge  $q_3q_4$  incident on the midpoint  $Q_T$  of edge  $q_1q_2$  creates third order edge diffraction ( $E_{Q_T}^{3d}$ ). Similarly, second order edge diffracted field ( $E_{Q_T}^{2d}$ ) from  $Q_T$  incident on  $Q_B$  creates third order edge diffraction ( $E_{Q_B}^{3d}$ ). These multiple edge diffracted fields are calculated using UTD technique of [3].

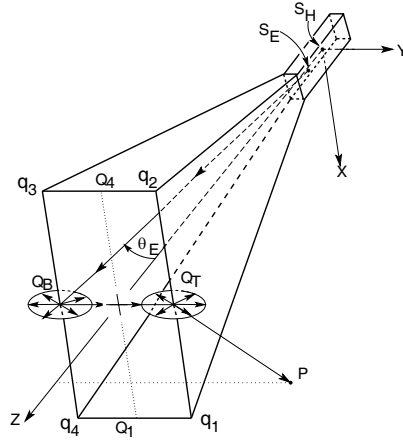


**Figure 5.** Multiple diffractions from  $E$ -edges.

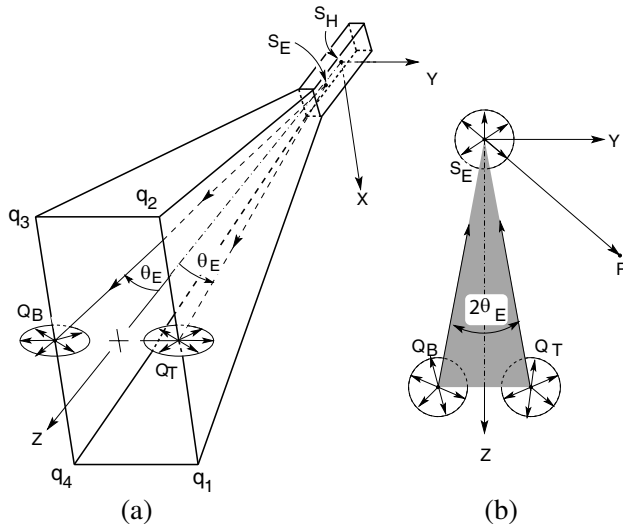


**Figure 6.** Second order wedge diffraction from apex  $S_E$ . (a) First order edge-diffractions due to the spherical source at  $S_E$  (b) Second order wedge diffractions due to the incidence of  $E$ -edge diffracted field.

First order diffracted field ( $E_{Q_T}^d$ ) from the midpoint  $Q_T$  of edge  $q_1q_2$  (see Fig. 6(a)) incident on the apex of the horn at  $S_E$  (see Fig. 6(b)) creates second order wedge diffraction ( $E_{Q_T}^{2dW}$ ). The apex of the horn is considered as a wedge of wedge angle  $2\theta_E$ . Similarly, first order diffracted field ( $E_{Q_B}^d$ ) from the point  $Q_B$  incident on the apex of

the horn at  $S_E$  creates second order wedge diffraction ( $E_{Q_B}^{2dW}$ ). These edge and wedge diffracted fields are calculated using UTD technique of [3].

Adding the above diffracted fields and using symmetry the  $E$ -plane radiation pattern is

$$\begin{aligned}
 E(P) = E^i(P) \Big|_{\text{for } |\theta_y| \leq \theta_E} \\
 + \left[ E_{Q_T}^d(P) + E_{Q_T}^{2d}(P) + E_{Q_T}^{3d}(P) \right] \Big|_{\text{for } 0^\circ \leq \theta_y \leq 180^\circ \text{ and } 270^\circ < \theta_y \leq 360^\circ} \\
 + \left[ E_{Q_B}^d(P) + E_{Q_B}^{2d}(P) + E_{Q_B}^{3d}(P) \right] \Big|_{\text{for } 0^\circ \leq \theta_y < 90^\circ \text{ and } 180^\circ \leq \theta_y \leq 360^\circ} \\
 + \left[ E_{Q_T}^{2dW}(P) + E_{Q_B}^{2dW}(P) \right] \Big|_{\text{for } \theta_E \leq \theta_y < 360^\circ - \theta_E}
 \end{aligned} \quad (2)$$

The computed radiation pattern using (2) is compared with the measurement shown in Fig. 7.

### 2.3. Analysis of $E$ -plane Horn Radiation Pattern by FEGTD Method

From (1), at  $\theta_x = \theta_H$ , incident field  $E^i$  is zero. So, the corner diffracted fields from end of the  $E$ -edges and  $H$ -edges are also zero. However, the slope of the incident field is nonzero. For grazing incidence, the edge slope diffraction coefficient in this case of hard boundary condition (BC) is also identically zero [21]. However, the edge slope diffraction coefficient for the soft BC case is non zero. The edge slope diffracted

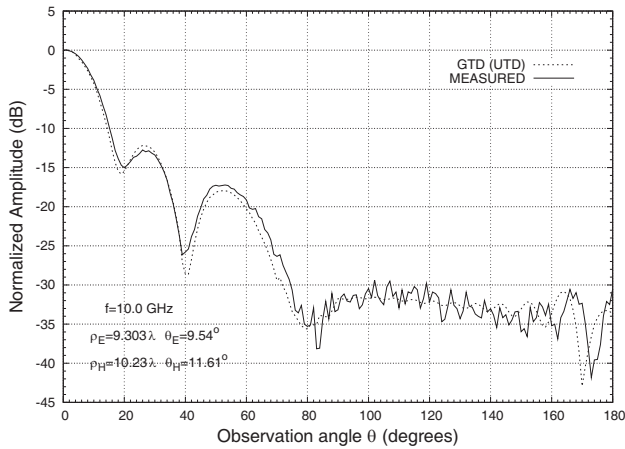


**Figure 7.**  $E$ -plane radiation pattern of a pyramidal horn antenna.



field for the soft BC case is much less than the edge diffracted field for the hard BC case at LRB directions. So the effects of corner slope diffracted field for the soft BC case are negligible in the LRB directions.

In order to incorporate the contributions of corner diffraction in the  $E$ -plane horn radiation pattern, we need to consider skewed rays incident on the  $E$ -edges (see Fig. 8). These rays appear to emanate from a point source located at  $S_E$ . The field diffracted from the  $E$ -edge at  $Q_2$  gives rise to the ray incident on the corner  $q_4$  at the end of adjacent  $H$ -edge  $q_1q_4$  and simultaneously at the end of the opposite  $E$ -edge  $r_3q_4$ . The corner  $q_4$  is first considered to be at one end of the half-plane  $q_3q_4S_H$  (see [13, Fig. 4]). The  $Y$ -component of the corner diffracted field  $E_{Q_2q_4}^{dH}(P)$  is obtained using the heuristic diffraction coefficient [22, Eq. (20)]. The spreading factor as well as phase function for the corner diffracted field is according to [22]. Next, the corner  $q_4$  is considered to be at the end of the half-plane  $q_1q_4S_E$  (see [13, Fig. 5]) and  $Y$ -component of the corner diffracted field  $E_{Q_2q_4}^{dE}(P)$  is obtained using the heuristic diffraction coefficient [22, Eq. (20)] Let,  $E_{Q_2q_4}^d(P)$  be the sum of fields  $E_{Q_2q_4}^{dE}(P)$  and  $E_{Q_2q_4}^{dH}(P)$  which is the contribution of corner  $q_4$  in  $E$ -plane radiation pattern. Similarly, the contributions of the others corners  $q_1$ ,  $q_2$  &  $q_3$  are also obtained.

On adding the corner diffracted field to the right hand side of (2)

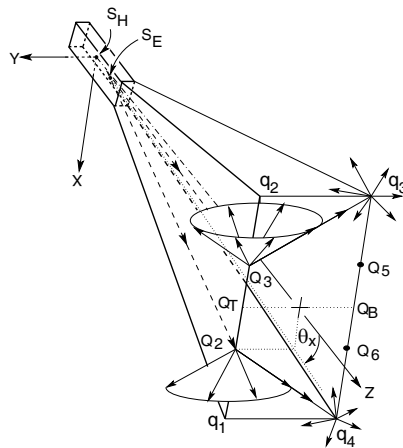


**Figure 8.**  $E$ -edge diffracted corner incident rays from a spherical source at  $S_E$ .

the  $E$ -plane radiation pattern using symmetry is

$$\begin{aligned}
 E2(P) = & E^i(P) \Big|_{\text{for } |\theta_y| \leq \theta_E} \\
 & + \left[ E_{Q_T}^d(P) + E_{Q_T}^{2d}(P) + E_{Q_T}^{3d}(P) \right] \Big|_{\text{for } 0^\circ \leq \theta_y \leq 180^\circ \text{ and } 270^\circ < \theta_y \leq 360^\circ} \\
 & + \left[ E_{Q_B}^d(P) + E_{Q_B}^{2d}(P) + E_{Q_B}^{3d}(P) \right] \Big|_{\text{for } 0^\circ \leq \theta_y < 90^\circ \text{ and } 180^\circ \leq \theta_y \leq 360^\circ} \\
 & + \left[ E_{Q_T}^{2dW}(P) + E_{Q_B}^{2dW}(P) \right] \Big|_{\text{for } \theta_E \leq \theta_y < 360^\circ - \theta_E} \\
 & + 2 \left[ E_{Q_{2q4}}^d(P) + E_{Q_{6q1}}^d(P) \right]
 \end{aligned} \tag{3}$$

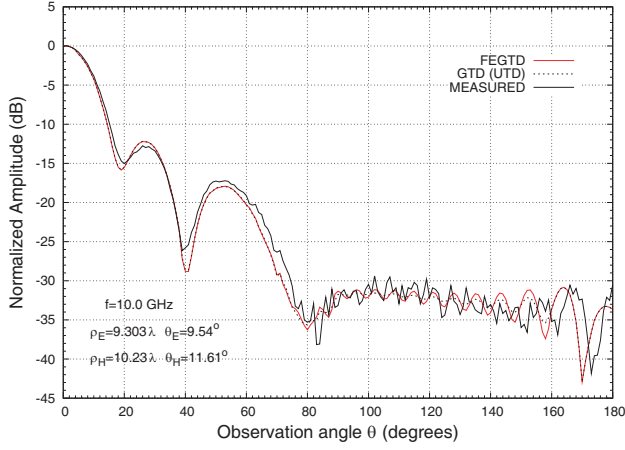


**Figure 9.**  $E$ -plane radiation pattern of a pyramidal horn antenna.

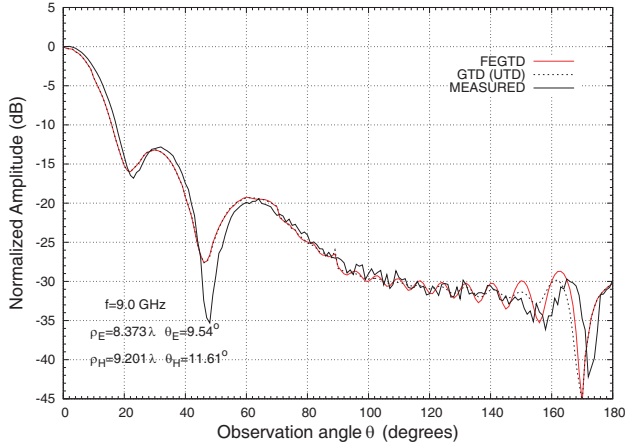


**Figure 10.**  $E$ -plane radiation pattern of a pyramidal horn antenna.

The computed radiation patterns using (3) are compared with the measurement and computed radiation patterns using GTD (UTD) technique (using (2)) shown in Figs. 9 & 10.

### 3. RESULTS AND DISCUSSIONS

$E$ -plane horn radiation pattern is computed using UTD with spherical source excitations. Firstly, diffracted fields from the  $E$ -edges due to the spherical source at the apex  $S_E$  are computed. Then multiple (double and triple) diffraction from the  $E$ -edges and double diffraction from the apex  $S_E$  due the  $E$ -edge diffracted field incidence on the apex are added. The computed pattern is compared with the measurement shown in Fig. 7. The computed pattern is well matched with the measurement in overall manner. The presence of ripples in the field pattern is predicted like in [12].

Skewed ray that result in corner diffraction is introduced and augmented  $E$ -plane horn radiation pattern is also computed. The results are compared with the radiation pattern using GTD (UTD) technique and measurements shown in Figs. 9 & 10. Corner diffraction was found to have significant influence on the  $E$ -plane horn radiation pattern in the LRB directions. The ripples in the measurement between the angle  $90^\circ$  and  $160^\circ$  are well predicted in compared with GTD (UTD) technique. As the far out ( $90^\circ$  to  $160^\circ$ ) side lobe levels in the  $E$ -plane vary around 25 to 40 dB the effect of corner diffraction is less compared to the  $H$ -plane case in [13], where the far out sidelobe levels were around 40 to 55 dB.

### ACKNOWLEDGMENT

This work was supported by the Ministry of Education, Science Technology (MEST) and Korea Institute for Advancement of Technology (KIAT) through the Human Resource Training Project for Regional Innovation under the Contract No. 20080702123415 and by the Brain Korea 21 Project, the School of Information Technology, KAIST in 2011.

### REFERENCES

1. Katz, D. S., M. J. Piket-May, A. Taflove, and K. R. Umashankar, "FDTD analysis of electromagnetic wave radiation from systems containing horn antennas," *IEEE Transactions on Antennas and Propagation*, Vol. 39, No. 8, 1203–1212, Aug. 1991.

2. Keller, J. B., "Geometrical theory of diffraction," *J. Opt. Soc. Amer.*, Vol. 52, 116–130, Feb. 1962.
3. Kouyoumjian, R. G. and P. H. Pathak, "A uniform geometrical theory of diffraction for an edge in a perfectly conducting surface," *Proceedings of the IEEE*, Vol. 62, No. 11, 1448–1461, Nov. 1974.
4. Ahluwalia, D. S., R. M. Lewis, and J. Boersma, "Uniform asymptotic theory of diffraction by a plane screen," *SIAM J. Appl. Math.*, Vol. 16, 783–807, 1968.
5. Lee, S. W. and G. A. Deschamps, "A uniform asymptotic theory of electromagnetic diffraction by a curved wedge," *IEEE Transactions on Antennas and Propagation*, Vol. 24, No. 1, 25–34, Jan. 1976.
6. Russo, P. M., R. C. Rudduck, and L. Peters, "A method for computing  $E$ -plane patterns of horn antennas," *IEEE Transactions on Antennas and Propagation*, Vol. 13, No. 2, 219–224, Mar. 1965.
7. Yu, J. S., R. C. Rudduck, and L. Peters, Jr., "Comprehensive analysis for  $E$ -plane of horn antennas by edge diffraction theory," *IEEE Transactions on Antennas and Propagation*, Vol. 14, No. 2, 138–149, Mar. 1966.
8. Yu, J. S. and R. C. Rudduck, " $H$ -plane pattern of a pyramidal horn," *IEEE Transactions on Antennas and Propagation*, Vol. 17, No. 5, 651–652, Sep. 1969.
9. Mentzer, C. A., L. Peters, Jr., and R. C. Rudduck, "Slope diffraction and its application to horns," *IEEE Transactions on Antennas and Propagation*, Vol. 23, No. 2, 153–159, Mar. 1975.
10. Narsimhan, M. S. and S. K. Rao, "GTD analysis of the near field patterns of pyramidal horns," *Proceedings of the IEEE*, Vol. 126, No. 12, 1223–1226, Dec. 1979.
11. Menendez, R. and S. W. Lee, "Analysis of rectangular horn antennas via uniform asymptotic theory," *IEEE Transactions on Antennas and Propagation*, Vol. 30, No. 2, 241–250, Mar. 1982.
12. Sanyal, S. and A. Bhattacharyya, "UAT analysis of  $E$ -plane near and far-field patterns of electromagnetic horn antennas," *IEEE Transactions on Antennas and Propagation*, Vol. 31, No. 5, 817–819, Sep. 1983.
13. Ali, M. and S. Sanyal, "A finite edge GTD analysis of the  $H$ -plane horn radiation pattern," *IEEE Transactions on Antennas and Propagation*, Vol. 58, No. 3, 969–973, Mar. 2010.
14. Boersma, J. and S. W. Lee, "High-frequency diffraction of a line-source field by a half-plane: Solutions by ray techniques," *IEEE*

- Transactions on Antennas and Propagation*, Vol. 25, No. 2, 171–179, Mar. 1977.
15. Boersma, J. and Y. Rahmat-Samii, “Comparison of two leading uniform theories of edge diffraction with the exact uniform asymptotic solution,” *Radio Science*, Vol. 15, No. 4, 1179–1194, Mar. 1980.
  16. Rahmat-Samii, Y. and R. Mittra, “Spectral analysis of high-frequency diffraction of an arbitrary incident field by a half plane — Comparison with four asymptotic techniques,” *Radio Science*, Vol. 13, No. 1, 31–48, Jan. 1978.
  17. Hsu, H.-T., F.-Y. Kuo, and H.-T. Chou, “Convergence study of current sampling profiles for antenna design in the presence of electrically large and complex platforms using fit-UTD hybridization approach,” *Progress In Electromagnetics Research*, Vol. 99, 195–209, 2009.
  18. He, Z.-L., K. Huang, and C.-H. Liang, “Analysis of complex antenna around electrically large platform using iterative vector fields and UTD method,” *Progress In Electromagnetics Research M*, Vol. 10, 103–117, 2009.
  19. Lertwiriayaprapa, T., P. H. Pathak, and J. L. Volakis, “An approximate UTD ray solution for the radiation and scattering by antennas near a junction between two different thin planar material slab on ground plane,” *Progress In Electromagnetics Research*, Vol. 102, 227–248, 2010.
  20. Kouyoumjian, R. G. and P. H. Pathak, “An analysis of the radiation from apertures in curved surfaces by the geometrical theory of diffraction,” *Proceedings of the IEEE*, Vol. 62, No. 11, 1438–1447, Nov. 1974.
  21. Pathak, P. H., “Techniques for high-frequency problem,” *Antenna Handbook — Theory, Application and Design*, Y. T. Lo and S. H. Lee (eds.), Ch. 4, 4-0–4-117, Van Nostrand Reinhold, New York, 1988.
  22. Joseph, P. J., A. D. Tyson, and W. D. Burnside, “An absorber tip diffraction coefficient,” *IEEE Transactions on Antennas and Propagation*, Vol. 36, No. 4, 372–379, Nov. 1994.